

Linear response to leadership, effective temperature and decision making in flocks

D. J. G. Pearce¹ and L. Giomi¹

¹*Instituut-Lorentz, Universiteit Leiden, P.O. Box 9506, 2300 RA Leiden, The Netherlands*

Large collections of autonomously moving agents, such as animals or micro-organisms, are able to “flock” coherently in space even in the absence of a central control mechanism. While the direction of the flock resulting from this critical behavior is random, this can be controlled by a small subset of informed individuals acting as leaders of the group. In this article we use the Vicsek model to investigate how flocks respond to leadership and make decisions. Using numerical simulations, we demonstrate that flocks display a linear response to leadership that can be cast in the framework of the fluctuation-dissipation theorem, identifying an “effective temperature” reflecting how promptly the flock reacts to the initiative of the leaders. The linear response to leadership also holds in the presence of two groups of informed individuals with competing interests, indicating that the flock’s behavioral decision is determined by both the number of leaders and their degree of influence.

The term “flocking” (or equivalently swarming, schooling, herding etc.) describes the ability of groups of living organisms to move coherently in space and time [1–3]. This behavior is ubiquitous in nature: it occurs in sub-cellular systems [4], bacteria [5], insects [6, 7], fish [8, 9], birds [10–14] and in general in nearly any group of individuals endowed with the ability to move and sense. This spectacular example of robustness has inspired science and technology in a two-fold way: on one hand scientists have focused their efforts in understanding the origin of a collective behavior found in systems of such an astonishing diversity [2]; on the other hand technologists have envisioned the possibility of implementing this form of social organization that spontaneously arises in living systems to construct flocks of devices that can work independently and yet collectively towards a common goal [15, 16].

A particularly interesting question in the context of collective behavior in biological and bio-inspired systems revolves around how groups respond to the leadership of a subset of individuals having pertinent information. In animals, such information might represent the location of a food source [17], a specific migration route [18], or a threat of which part of the group is unaware, such as a predator only visible to a minority of individuals [19]. In biomimetic systems, on the other hand, this might consist of a set of instructions related with the group task. The response of schooling fish to leadership has represented, in particular, the focus of several empirical studies. This is thanks to the possibility of training fish to swim toward a specific target, expect food at a given time or location [20–22] or the ability to insert remote-controlled replica animals [23, 24], thus acting as leaders for the remaining fish. While varying in the details, these studies have demonstrated that large groups of individuals are able to adopt the behavior of an informed subset. The statistical mechanics of leadership and decision making in animal groups has been systematically investigated by Couzin and coworkers in a series of seminal works [17, 24–26]. Using a combination of experiments and numerical simulations based on self-propelled particles models, they

showed that communities of collectively moving individuals are able to make consensus decisions in the presence of a small minority of unorganized informed individuals. Furthermore, they demonstrated that when two informed subsets with competing behaviors are introduced, the group selects the behavior of the larger informed subset with an accuracy that increases with the number of uninformed individuals [17].

The generality and the robustness of these results have acted as a stimulus to identify a generic mechanism behind leadership and decision making in systems of collectively moving individuals [27, 28]. Yet, whether it is possible to identify the basic laws governing the response of a group to leadership, is still unclear.

In order to gain insight on this problem, we present here a linear response analysis of a model flock whose dynamics is described by the Vicsek model with angular noise [29]. We study how a collection of flocking agents respond to the leadership of a randomly selected subset of the entire flock that is biased to turn toward a specific direction. Using numerical simulations, we demonstrated that the system’s response to leadership can be cast in the framework of the fluctuation-dissipation theorem, upon introducing an “effective temperature” proportional to the ratio between the correlation and response functions and generally dependent on the system density, velocity and noise. Remarkably, both the density and velocity dependence disappear at large densities, revealing a universal linear dependence of the effective temperature on the noise variance. We then apply this approach to the case wherein the flock must choose between two subsets of leaders with competing interests, identifying again a linear response to the total perturbation applied by both groups. In this case, however, the flock behavioral decision is determined by both the number of leaders and their degree of influence, so that a small subgroup of particularly influential informed individuals can overrule a larger subset of less influential informed individuals.

Let us consider the Vicsek model subject to angular white noise [29]. The system consists of N individuals traveling at velocity $\mathbf{v}_i = v_0(\cos \theta_i, \sin \theta_i)$, with

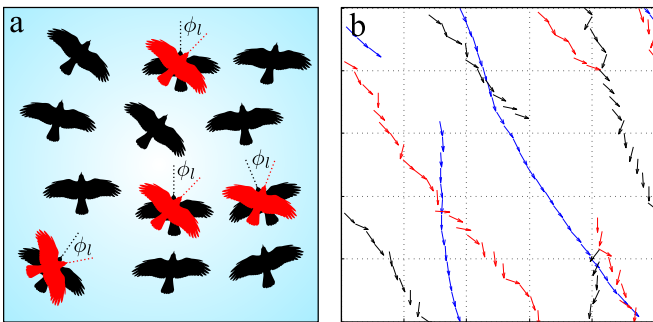


FIG. 1. (a) Example of how the perturbation is applied to the flock, in this sketch $N_l = 4$ leaders out of $N = 12$ individuals turn by an angle ϕ_l , thus changing their direction of motion from the black to the red dashed line. (b) A snapshot of a typical simulation; shown is the trajectory of one of the perturbed particles (red), a normal unperturbed particle (black) and a tracer particle inserted into the system that has $\eta = 0$ (blue). This represents 200 consecutive time steps from a simulation of $N = 1600$ particles with $\rho = 16$, $\eta = 0.25$, $N_l = 50$ and $\phi_l = 0.1$.

$i = 1, 2 \dots N$ and v_0 a constant speed, on a square $L \times L$ periodic two-dimensional domain. At each time step each individual takes the average direction of those within some pre-defined radius R as its new direction. Thus:

$$\mathbf{r}_i(t + \Delta t) = \mathbf{r}_i(t) + \mathbf{v}_i(t) \Delta t, \quad (1a)$$

$$\theta_i(t + \Delta t) = \langle \theta_i(t) \rangle_R + \xi_i, \quad (1b)$$

where \mathbf{r}_i is the position of the i -th individual at time t , ξ_i a uniformly distributed random angle in the range $[-\eta, \eta]$ and $\langle \theta_i \rangle_R = \arctan(\langle \sin \theta_i \rangle_R / \langle \cos \theta_i \rangle_R)$ is the average orientation of all the individuals within a distance R from \mathbf{r}_i , including the i -th one. Following a classic convention, we set $\Delta t = R = 1$, thus choosing Δt as unit of time and the interaction range R as unit of distance.

In order to study the linear response of the flock to a perturbation, we consider the system polarization vector, defined as:

$$\mathbf{P}(t) = \frac{1}{v_0 N} \sum_{i=1}^N \mathbf{v}_i(t); \quad (2)$$

The magnitude $P = |\mathbf{P}|$ serves as an order parameter and allows to distinguish the isotropic (where $P = 0$) and flocking ($P > 0$) phase. The unit vector $\mathbf{p} = \mathbf{P}/P$, on the other hand, represents the global direction of the flock. Now, deeply in the order phase (i.e $P \sim 1$), \mathbf{p} changes very slowly and the polarization vector randomly precesses along the unit circle (Supplementary Movie S1). To quantify this process we introduce a discrete analog of curvature in the flock trajectory:

$$\kappa(t) = [\mathbf{p}(t-1) \times \mathbf{p}(t)] \cdot \hat{\mathbf{z}}. \quad (3)$$

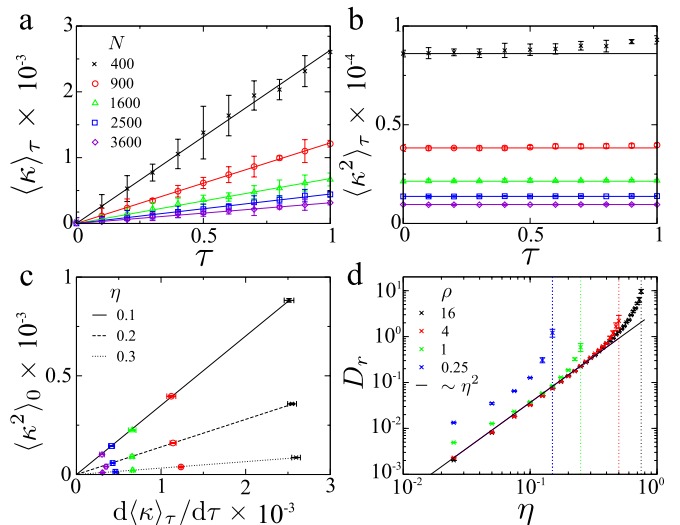


FIG. 2. a) The mean response curvature, $\langle \kappa \rangle_\tau$, of the trajectory of the flock is linear with the degree of perturbation, τ . b) Conversely, the mean squared curvature, $\langle \kappa^2 \rangle_\tau$, remains constant for small τ values. c) The mean squared curvature is linear with the gradient of the response, $d\langle \kappa \rangle_\tau / d\tau$. d) The gradient of plot (c) corresponds to the rotational diffusion coefficient, D_r , and follows a power law relationship with the magnitude of the noise for flocks at high density in the ordered phase. The dotted lines in plot (d) correspond to the approximate position of the critical point of the phase transition identified in the Supplementary Information.

In the absence of any rotational bias, the flock is equally likely to turn left or right, hence $\langle \kappa \rangle_0 = 0$ and $\langle \kappa^2 \rangle_0 \neq 0$, where the brackets represent a time average in the unperturbed system. Next, let us consider a subset of $N_l \leq N$ randomly chosen “informed individuals” within the flock, who are biased to turn toward a specific direction. For each of them, Eq. (1b) is replaced by $\theta_i(t + \Delta t) = \phi_l + \langle \theta_i(t) \rangle_R + \xi_i$, where ϕ_l is a constant angular displacement representing the “degree of influence” of each informed individual within its neighborhood. While there are other ways to introduce an internal bias in the Vicsek model [30, 31], this is possibly the one that most closely resembles maneuvers in real flocks. The product $\tau = \phi_l N_l$ is analogous to an *effective torque* that is able to bend the trajectory of flock toward the left or right, depending on the sign of ϕ_l (see Fig. 1 and Supplementary Movie S2).

In order to investigate the influence of the informed individuals in the general behavior of the flock, we have performed various numerical simulations (see the Supplementary Information for numerical details). Fig. 2a,b shows the first and second moment in the probability distribution of κ as a function of τ . As a consequence of the directional bias introduced by the informed individuals, the trajectory of the flock acquires a non-zero mean curvature that grows linearly with τ : i.e. $\langle \kappa \rangle_\tau \sim \tau$, where $\langle \dots \rangle_\tau$ represent a time average in the presence of an ef-

fective torque τ . It is worth stressing that the linear response of the flock to leadership is not independently governed by the number of leaders N_l or their influence ϕ_l , but rather by their product τ , so that doubling the number of leaders in the group is equivalent to keeping their number fixed, while doubling their influence (Supplementary Information Fig. 3). The slope $d\langle\kappa\rangle_\tau/d\tau$ depends, in general, on all the parameters in the model, including the flock population N , size L , velocity v_0 and noise η . The second moment $\langle\kappa^2\rangle_\tau$ is, on the other hand, independent on τ for small τ values and plateaus to the curvature variance $\langle\kappa^2\rangle_0$ of the unbiased flock (Fig. 2b). Remarkably, the ratio between $d\langle\kappa\rangle_\tau/d\tau$ and $\langle\kappa^2\rangle_0$ depends on the flock population and size only through its density $\rho = N/L^2$ (Fig. 2c). This allows us to formulate the following linear response relation for the Vicsek model subject to the leadership of a subset of informed individuals:

$$\frac{d\langle\kappa\rangle_\tau}{d\tau} = \frac{1}{2D_r} \langle\kappa^2\rangle_0. \quad (4)$$

where D_r is an effective rotational diffusion coefficient, generally dependent on the system density, noise and particle velocity. In order to gain insight about the dependence of D_r on the remaining free parameters of the system, we have repeated the previous analysis for various v_0 , ρ and η values (Fig. 2d and Supplementary Information Fig. 4) and find that, surprisingly, the density and velocity dependence disappears at high densities, revealing a universal linear dependence of D_r on the variance of noise: $D_r \sim \eta^2$.

Some comments are in order. Eq. (4) is a special case of the fluctuation-dissipation theorem (FDT), with a collective effective temperature $T_{\text{eff}} \sim D_r$. In the realm of active matter, the possibility of an effective temperature and a generalized FDT has been discussed for both dilute and dense phases [30–37], sometimes with contradictory results. Czirók *et al.* [30] analyzed the response of a Vicsek flock to a spatially uniform ordering field and found no evidence of a fluctuation-dissipation relation. This was instead identified by Chaté and coworkers [31], who considered an external field coupled with the local average polarization. The effective temperature resulting from this relation, however, varies in the parameter space. More recently, Levis and Berthier [37] have investigated the response to an external perturbation of a system of self-propelled disks and found that, while the FDT is generally violated, a collective effective temperature does emerge at high density, in proximity of a non-equilibrium glass transition. This scenario, partially anticipated by the mean-field analysis reported in Ref. [35], was ascribed to a suppression of the short wavelength fluctuations in favor of the long-wavelength collective modes appearing at the onset of the glass transition. Our findings, indicate that a special form of the FDT, with an effective temperature only dependent on

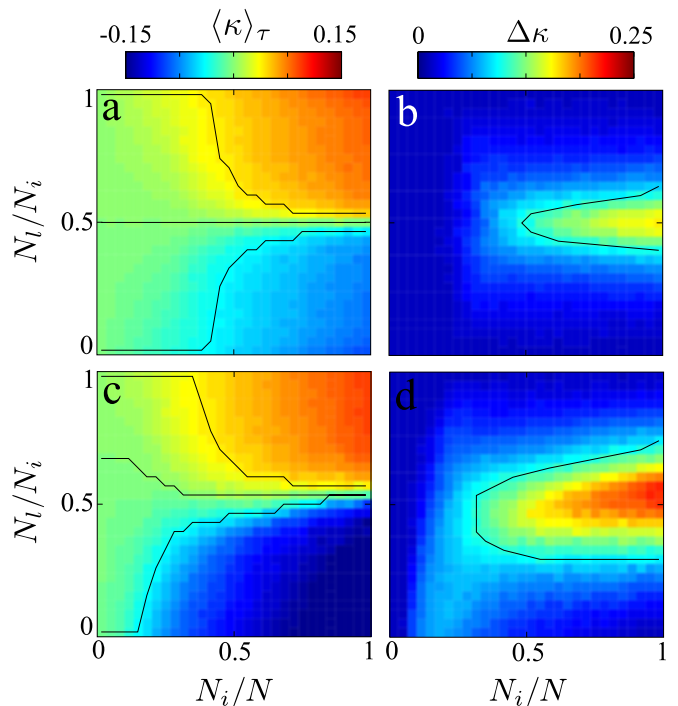


FIG. 3. Induced mean (a,c) and standard deviation (b,d) curvature in the motion of the flock due to competing subsets of informed individuals. Here N_l and N_r individuals giving the flock a positive and negative curvature respectively, with $N_i = N_l + N_r$. (a,b) When the competing subsets have equal and opposite influence ($\phi_l = -\phi_r$) the resulting curvature is of the same sign as the largest informed subset, and the inclusion of uninformed individuals reduces the standard deviation of the curvature. (c,d) When $\phi_r = -2\phi_l$ the resulting curvature is distorted and the relative sizes of the informed subsets is no longer sufficient to predict the curvature. The black lines in (a,c) show $\langle\kappa\rangle_\tau = -0.04, 0, +0.04$ and in (b,d) show $\langle\kappa^2\rangle_\tau = 0.1$, all simulations here are done with $N = 900$, $\rho = 4$, $v_0 = 0.1$, $\phi_l = 0.1$.

the variance of angular noise, can be identified in the Vicsek model subject to the leadership of a subset of informed individuals, as long as the system is sufficiently dense. As in the case of self-propelled disks [35], this behavior appears to stem from a suppression of short wavelength fluctuations at high densities, even in the absence of a glassy phase.

We next turn our attention to how flocks make decisions. As mentioned earlier, combined experimental and theoretical studies on schooling fish [17, 24–26] have demonstrated that, in the presence of competing interests (i.e. such as swimming toward two different targets), the group decides to conform to the behavior of the largest minority with an accuracy that increases with the number of uninformed individuals. Our approach allows us to study this result in a system where the response can vary continuously. To this purpose, we have introduced a second subset of N_r individuals with an angular displacement $\phi_r = -\phi_l$, so that $N_i = N_l + N_r$ is now the

total number of informed individuals and the flock must decide between two competing informed subsets. Fig. 3a shows that the sign of the resulting curvature of the flock is dictated by the largest subset of informed individuals; this is true even when the competing subsets in the flock are of similar size, $N_l \approx N_r$. However, as the number of informed individuals becomes large, $N_i \approx N$, the standard deviation in the curvature, $\Delta\kappa = \sqrt{\langle\kappa^2\rangle_\tau - \langle\kappa\rangle_\tau^2}$, significantly increases and the flock becomes less efficient at selecting the correct behavior. This is because when most individuals in the flock are leaders, with either a positive or negative curvature, there are few followers to average out the competing effects.

Due to the nature of the perturbation (and response) we have introduced we are not restricted to making binary decisions between subsets of equally influential informed individuals, indeed the total perturbation applied (and the measured response) can be varied continuously. Fig. 3c shows the response of a flock when $\phi_r = -2\phi_l$. Here we see again that the presence of uninformed individuals reduces the standard deviation, but the resulting curvature is no longer symmetric around $N_l = N_r$. Hence a smaller but sufficiently influential subgroup can dictate the sign of the curvature of the flock trajectory.

The asymmetry in Fig. 3c shows that the response to competing subsets of leaders is not dependent only on the size of the subsets, but also on their influence. As was shown earlier, the response of the flock varies continuously and is a function of the total effective torque τ . This result can be extended in the presence of two competing subsets of informed individuals upon introducing a generalized effective torque $\tau = \phi_l N_l + \phi_r N_r$. To verify this we fixed the relative size of the informed subsets ($N_r - N_l$) and varied their relative influence ϕ_l/ϕ_r achieving a range of responses, see Fig. 4a. By normalizing the response curvature by this newly defined τ we find that all the results fall onto the same value, Fig. 4b. This confirms that the linear response to leadership extends to competing subgroups of leaders implying all these flocks are at the same effective temperature. Hence flocks do not merely select the behavior of the largest subset of informed individuals, but rather the resulting behavior is the response to the total influence of both subsets on the flocks (the same result can be achieved by fixing ϕ_l/ϕ_r and varying $N_r - N_l$, see Supplementary Information Fig. 5).

In conclusion, we have investigated how a model flock, whose dynamics is described by the Vicsek model, respond to the leadership of a subset of informed individuals. Using numerical simulations, we have demonstrated that the process obeys to a special form of the FDT, with an emerging effective temperature that depends uniquely on the variance of noise for sufficiently dense systems. The linear response to leadership also holds in the presence of two subgroups of informed individuals with competing interests, in this case the flock behavioral decision

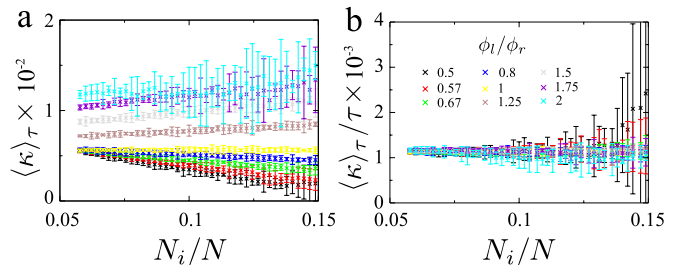


FIG. 4. a) Resulting curvature of flocks with $N_l - N_r$ fixed and varying values of ϕ_r . As is clear here the resulting curvature is not just the function of the relative sizes of the informed subsets, rather it is the total torque. b) The ratio between the resulting curvature and the total torque is constant across all simulations, indicating this is the only important parameter here. All simulations here are done with $N = 900$, $\rho = 4$, $v_0 = 0.1$, $\phi_l = 0.1$, $N_l - N_r = 50$.

is determined by both the number of leaders and their degree of influence. So that a small subgroup of particularly influential informed individuals can overrule a larger subset of less influential informed individuals.

We would like to thank Matthew Turner and Denis Bartolo for helpful discussions while producing this work. This work is supported by The Netherlands Organization for Scientific Research (NWO/OCW).

-
- [1] C. W. Reynolds, *Comp. Graph.* **21**, 25 (1987).
 - [2] T. Vicsek and A. Zafeiris, *Phys. Rep.* **517**, 71 (2012).
 - [3] I. Giardina, *HFSP J* **2**, 205 (2008).
 - [4] V. Schaller, C. Weber, C. Semmrich, E. Frey, and A. R. Bausch, *Nature* **467**, 73 (2010).
 - [5] F. Peruani, J. Starruß, V. Jakovljevic, L. Søgaard-Andersen, A. Deutsch, and M. Bär, *Phys. Rev. Lett.* **108**, 098102 (2012).
 - [6] V. Guttal, P. Romanczuk, S. J. Simpson, G. A. Sword, and I. D. Couzin, *Ecol. Lett.* **15**, 1158 (2012).
 - [7] S. Bazazi, J. Buhl, J. J. Hale, M. L. Anstey, G. A. Sword, S. J. Simpson, and I. D. Couzin, *Curr. Biol.* **18**, 735 (2008).
 - [8] J. E. Herbert-Read, A. Perna, R. P. Mann, T. M. Schaerf, D. J. Sumpter, and A. J. Ward, *Proc. Natl. Acad. Sci. U.S.A.* **108**, 18726 (2011).
 - [9] O. A. Misund, A. Aglen, and E. Frønæs, *ICES J. Mar. Sci.* **52**, 11 (1995).
 - [10] M. Ballerini, R. C. N. Cabibbo, A. Cavagna, E. Cisbani, I. Giardina, and V. Zdravkovic, *Proc. Natl. Acad. Sci. U.S.A.* **105**, 1232 (2008).
 - [11] D. J. Pearce, A. M. Miller, G. Rowlands, and M. S. Turner, *Proc. Natl. Acad. Sci. U.S.A.* **111**, 10422 (2014).
 - [12] A. Cavagna, I. Giardina, and F. Ginelli, *Phys. Rev. Lett.* **110**, 168107 (2013).
 - [13] W. Bialek, A. Cavagna, I. Giardina, T. Mora, E. Silvestri, M. Viale, and A. M. Walczak, *Proc. Natl. Acad. Sci. U.S.A.* **109**, 4786 (2012).
 - [14] D. J. Pearce and M. S. Turner, *New J. Phys.* **16**, 082002 (2014).

- [15] L. Giomi, N. Hawley-Weld, and L. Mahadevan, *Proc. R. Soc. A* **469** (2013), 10.1098/rspa.2012.0637.
- [16] M. Rubenstein, A. Cornejo, and R. Nagpal, *Science* **345**, 795 (2014).
- [17] I. D. Couzin, C. C. Ioannou, G. Demirel, T. Gross, C. J. Torney, A. Hartnett, L. Conradt, S. A. Levin, and N. E. Leonard, *Science* **334**, 1578 (2011).
- [18] G. Dell’Ariccia, G. Dell’Omo, D. P. Wolfer, and H.-P. Lipp, *Animal Behaviour* **76**, 1165 (2008).
- [19] A. J. Ward, J. E. Herbert-Read, D. J. Sumpter, and J. Krause, *Proc. Natl. Acad. Sci. U.S.A.* **108**, 2312 (2011).
- [20] S. G. Reebs, *Anim. Behav.* **59**, 403 (2000).
- [21] J. Krause, D. Hoare, S. Krause, C. Hemelrijk, and D. Rubenstein, *Fish Fish.* **1**, 82 (2000).
- [22] C. Leblond and S. G. Reebs, *Behaviour* **143**, 1263 (2006).
- [23] J. J. Faria, J. R. Dyer, R. O. Clément, I. D. Couzin, N. Holt, A. J. Ward, D. Waters, and J. Krause, *Behav. Ecol. Sociobiol.* **64**, 1211 (2010).
- [24] A. J. Ward, D. J. Sumpter, I. D. Couzin, P. J. Hart, and J. Krause, *Proc. Natl. Acad. Sci. U.S.A.* **105**, 6948 (2008).
- [25] I. D. Couzin, J. Krause, N. R. Franks, and S. A. Levin, *Nature* **433**, 513 (2005).
- [26] D. J. Sumpter, J. Krause, R. James, I. D. Couzin, and A. J. Ward, *Curr. Biol.* **18**, 1773 (2008).
- [27] A. B. Kao, N. Miller, C. Torney, A. Hartnett, and I. D. Couzin, *PLoS Comput Biol* **10**, e1003762 (2014).
- [28] V. Guttal and I. D. Couzin, *Commun. Integr. Biol.* **4**, 294 (2011).
- [29] T. Vicsek, A. Czirók, E. Ben-Jacob, I. Cohen, and O. Shochet, *Phys. Rev. Lett.* **75**, 1226 (1995).
- [30] A. Czirók, H. E. Stanley, and T. Vicsek, *J. Phys. A-Math. Gen.* **30**, 1375 (1997).
- [31] H. Chaté, F. Ginelli, G. Grégoire, and F. Raynaud, *Phys. Rev. E* **77**, 046113 (2008).
- [32] D. Loi, S. Mossa, and L. F. Cugliandolo, *Phys. Rev. E* **77**, 051111 (2008).
- [33] S. Wang and P. G. Wolynes, *J. Chem. Phys.* **135**, 051101 (2011).
- [34] D. Loi, S. Mossa, and L. F. Cugliandolo, *Soft Matter* **7**, 10193 (2011).
- [35] L. Berthier and J. Kurchan, *Nat. Phys.* **9**, 310 (2013).
- [36] G. Szamel, *Phys. Rev. E* **90**, 012111 (2014).
- [37] D. Levis and L. Berthier, *Europhys. Lett.* **111**, 60006 (2015).

SUPPLEMENTARY INFORMATION

Simulation Methods

All simulations and analysis were performed using code written by the D.J.G.Pearce in C++. The code follows a slightly modified version of the original Vicsek model outlined in [29]. All simulations were pre-equilibrated by a minimum of 10 000 time steps, significantly longer than the autocorrelation time in the curvature of an unperturbed flock.

Each point in Fig. 2a,b (main text) corresponds to an average calculated over simulation of 150 000 time steps with $v_0 = 0.1$, $\rho = N/L^2 = 4$, $\eta = 0.1$. 11 such simulations were used to perform the regressions for each point displayed in Fig. 2c (main text). 6 such regressions were then created in order to create each point in Fig. 2d (main text). This is also true for all points represented in Supplementary Figs. 3&4.

Each point on the color plots in Fig. 3 (main text) corresponds to an average over a simulation of 150 000 time steps with 29 increments in the y direction and 30 increments in the x direction. The parameters used were $v_0 = 0.1$, $\rho = N/L^2 = 4$, $N = 900$, $\eta = 0.2$.

Each point in Fig. 4 (main text) corresponds to an average over a simulation of 150 000 time steps with $v_0 = 0.1$, $\rho = N/L^2 = 4$, $N = 900$, $\eta = 0.2$.

Unless stated otherwise, all simulations are performed at $v_0 = 0.1$, $\rho = N/L^2 = 4$.

Location of an steady state

What we shall consider the steady state with respect to the polarization vector, P . Much care must be taken when defining this steady state due to the nature of the phase transition of the Vicsek model. There has been much debate over the nature of the order transition in the Vicsek model but the current consensus is that it is of a discontinuous nature. This suggests that close to the transition, the state of the flock is not well defined by the parameters of the model as there are some regions of phase space where there are degenerate behaviors. For this reason we shall concentrate on the ordered phase of the flock, having both low noise and high density. Our method would indeed not be possible in the disordered phase of the flock as a well defined polarization is required in order for it to be possible to measure its precession.

For clarity we have included a representation of the order transition at the densities we are considering, that is $\rho = 0.25$, $\rho = 1$, $\rho = 2$ and $\rho = 4$ ($\rho = N/L^2$), Supplementary Fig .1. Supplementary Fig .1a gives an indication of the magnitude of the polarization of the flock in the regions we are considering. The sharp decrease in the binder cumulant, Supplementary Fig .1c, and the

location of the maximum in the susceptibility, Supplementary Fig .1c will be used to estimate the location of the critical point, η_c . For noise amplitudes above η_c we do not expect to reliably obtain a rate of precession of the polarization since in the infinite size limit the magnitude of the polarization is expected to diminish to zero, making any precession meaningless, therefore we restrict our analysis to the case when $\eta < \eta_c$. We see that as the noise amplitude approaches the critical point, $\langle \kappa^2 \rangle_0$ quickly diverges, which would also make the analysis impossible.

Diffusive nature of the polarization vector.

To confirm the diffusive nature of the polarization vector we simulated flocks at varying values of noise and observed how the polarization vector precessed with no applied perturbation. For short times the angle of the polarization vector appears to take a random walk in 1D, Supplementary Fig. 2a, the distribution of the steps closely follows a gaussian distribution, Supplementary Fig. 2b. In the long time limit the angle of the polarization vector clearly takes on a diffusive nature, $\langle \Delta\theta^2 \rangle_0 \sim \Delta t$, see Supplementary Fig. 2c.

Justification of $\tau = \phi_l N_l$

When adjusting the total applied perturbation in Fig. 2 (main text) we adjust the number of particles that the perturbation is applied to, N_l , while keeping ϕ_l , constant. Supplementary Fig. 3 clearly shows that this is equivalent to adjusting the size of the perturbation by keeping N_l constant and varying ϕ_l . Both methods of applying the perturbation give the same result.

Independence of particle speed, v_0

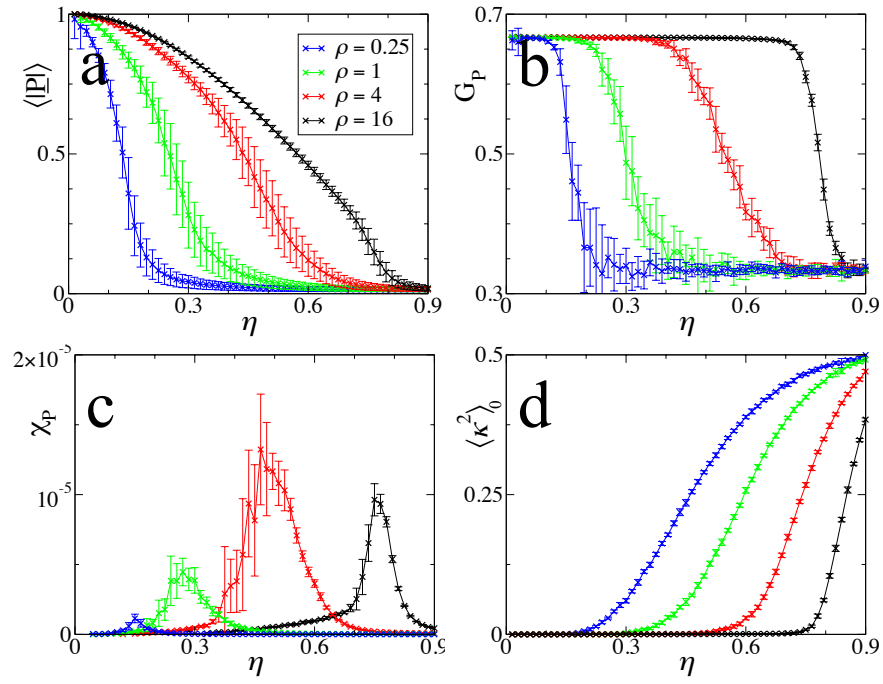
The observed rotational diffusion coefficient does not depend on the particle velocity, Supplementary Fig. 4. This may not be the case when $v_0 \gg R$ and the arrangement of the flock is effectively randomized between time steps or $v_0 \sim 0$ and the arrangement becomes effectively fixed at accessible timescales. Here we choose to stay within the regime that recreates flocking like behavior similar to the collective motion of animals.

Varying the relative size of informed subsets

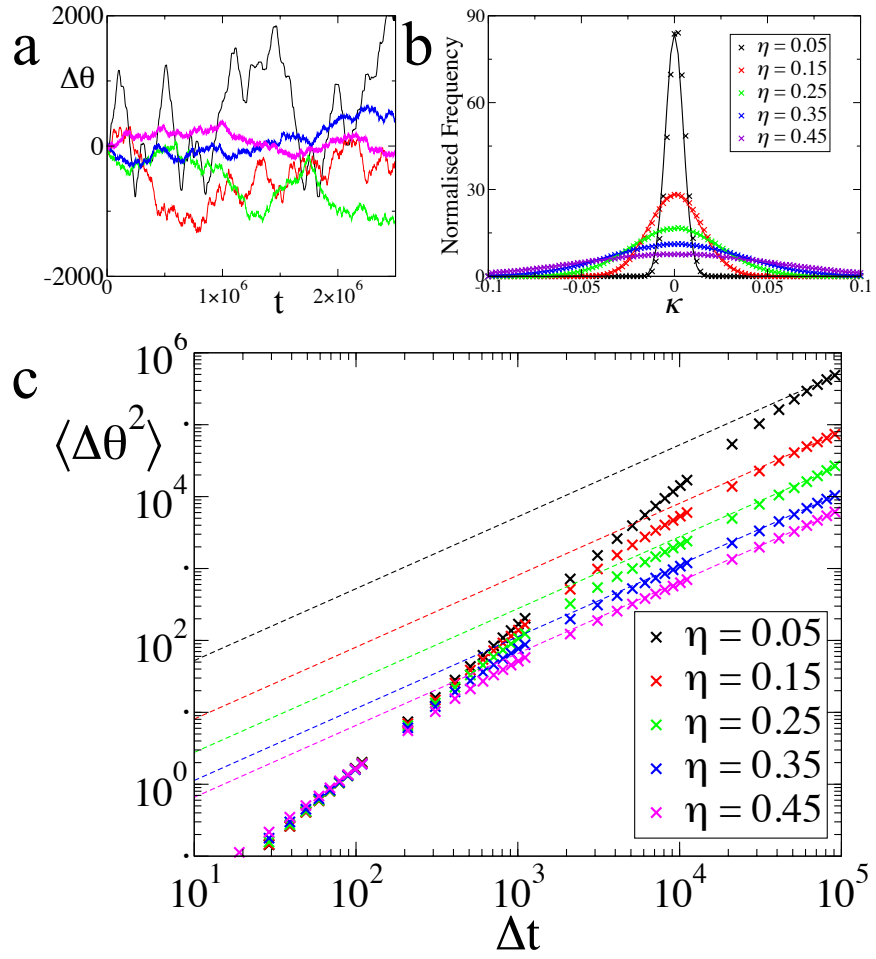
Fig. 4 (main text) shows that the response of a flock to the influence of two competing subsets is linear with the combined perturbation of the competing subsets. The relative magnitude of perturbation due to each to the two

sets can be varied by adjusting the ratio ϕ_l/ϕ_r (shown in Fig. 4 (main text)), or by adjusting their relative size $N_l - N_r$. Supplementary Fig. 5 mirrors the analysis performed in Fig. 4 (main text) but now fixing ϕ_l/ϕ_r and adjusting $N_l - N_r$ to recreate the same result. Addition-

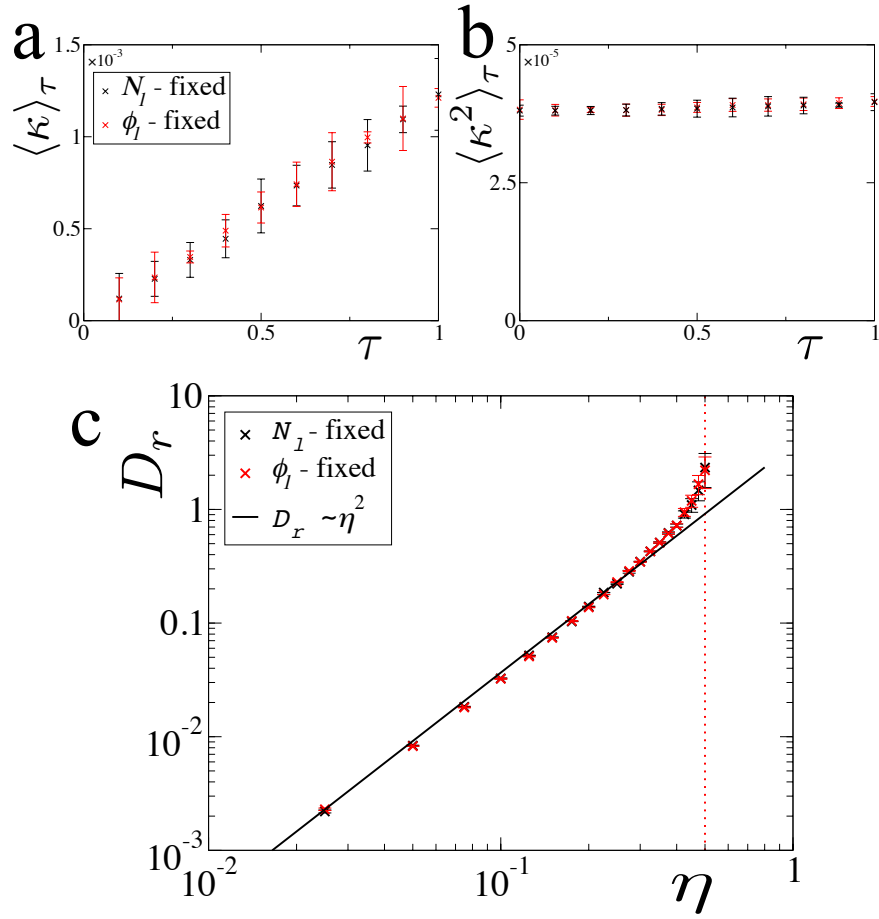
ally we see here that the result remains true even when τ changes sign, this crossover corresponds to the regions of Supplementary Fig. 5b where the normalized curvature appears to diverge since τ is very small.



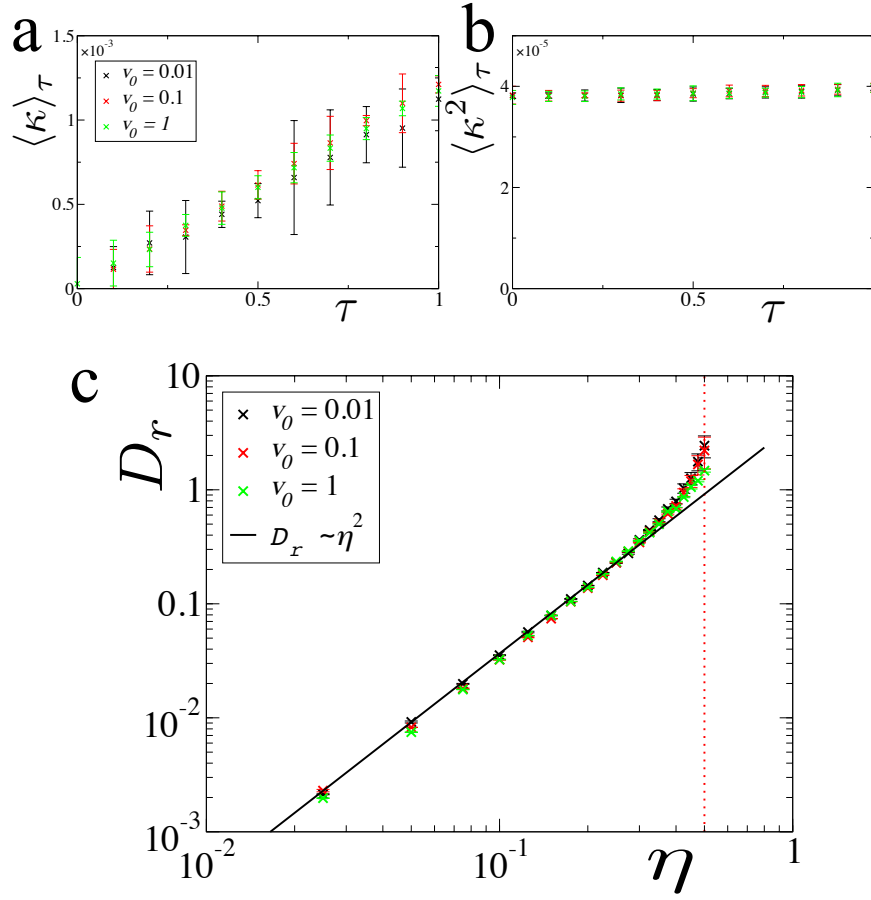
Supplementary FIG 1. (a) The magnitude of the polarization vector $|P|$ (a), Binder cumulant G_P (b), susceptibility χ_P (c) and mean square rate of precession of the polarization of the flock, $\langle \kappa^2 \rangle_0$ (d) as the noise is adjusted through the order transition. The different colours correspond to the different densities at which the simulations were performed. All results here are for systems of $N = 3600$ particles with $v_0 = 0.1$ and the data was taken over 150,000 time steps after a 10 000 step relaxation period. The data presented here is only to show the location and proximity of the critical point of the Vicsek flock at these sizes, and is not a exploration of the nature of the transition.



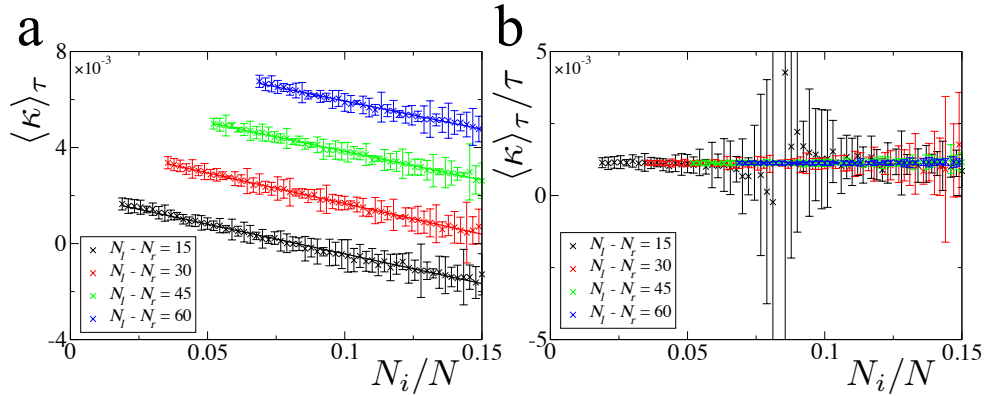
Supplementary FIG 2. (a) Angle of the polarization vector over the course of a simulation. b) The distribution of the angular displacement at each time step closely follow a gaussian with a spread that depends on the noise value. c) Mean squared angular displacement of the polarization vector is linear in time in the long time limit, revealing a diffusive nature. All results here are for systems of $N = 400$ particles with $\rho = 4$ and the data was taken over 3 200 000 time steps after a 150 000 step relaxation period.



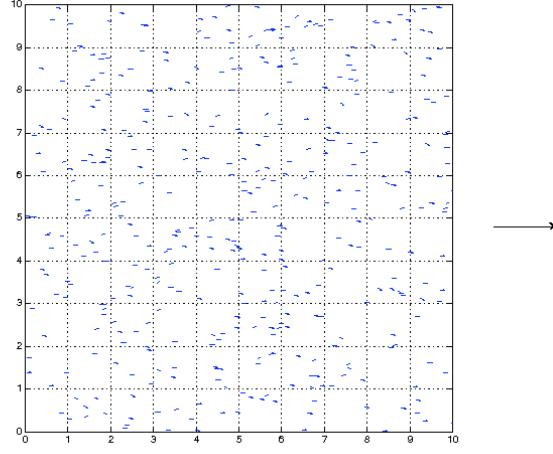
Supplementary FIG 3. (a) Response curvature of the flock to the total torque applied and (b) the mean square response and (c) rotational diffusion coefficient depend only on the total applied torque, τ , regardless of whether it is adjusted by varying N_l or ϕ_l . (a) and (b) both show the results for $N = 900$ and $\eta = 0.1$. The black and red points represent simulations where $N_l = 10$ and $\phi_l = 0.1$, respectively. All results here are for particles with $\rho = 4$, $v_0 = 0.1$ and the data was taken over 150 000 time steps after a 10 000 step relaxation period.



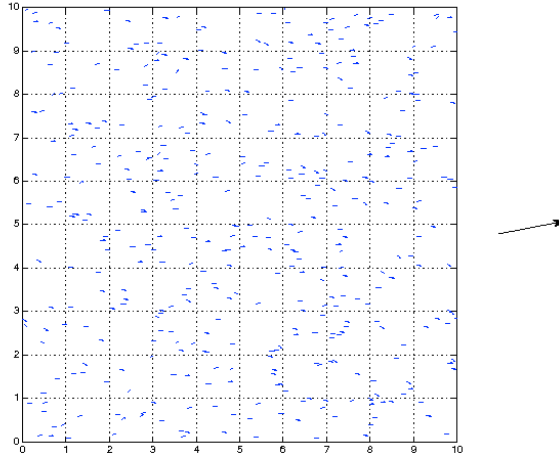
Supplementary FIG 4. (a) Response curvature of the flock to the total torque applied, (b) the mean square response and (c) diffusion coefficient are independent of the value of v_0 . (a) and (b) both show the results for $N = 900$ and $\eta = 0.1$. All results here are for systems with $\rho = 4$ and the data was taken over 150 000 time steps after a 10 000 step relaxation period.



Supplementary FIG 5. a) The responding curvature of a flock with two competing subsets of leaders, N_l with influence ϕ_l and N_r with influence ϕ_r , here we have set $\phi_r = -1.5\phi_l$. When the curvature is normalized by the total torque applied to the system all simulations give the same response, hence the flock is acting like a thermal bath with a linear response to leadership. All results here are for systems with $N = 900$, $v_0 = 0.1$, $\rho = 4$ and the data was taken over 150 000 time steps after a 10 000 step relaxation period.



Supplementary Movie 1. A flock following the standard unperturbed Vicsek model. Alongside the movie is the normalized polarization vector. The normalized polarization is on a random walk on the unit circle. The simulation is performed with $N = 400$, $v_0 = 0.1$, $R = 1$, $\rho = 4$, $\eta = 0.15$, $N_l = 0$ and $\phi_l = 0$ resulting in a total perturbation of $\tau = 0$.



Supplementary Movie 2. A flock following the standard Vicsek model with an angular perturbation as introduced in the main text. Alongside the movie is the normalized polarization vector. Over the course of the simulation the normalized polarization vector rotates around 2π . The simulation is performed with $N = 400$, $v_0 = 0.1$, $R = 1$, $\rho = 4$, $\eta = 0.15$, $N_l = 10$ and $\phi_l = 0.1$ resulting in a total perturbation of $\tau = 1$.